Photocopying Living Chains. 1. Steady-State

Erdem Karatekin,[†,‡] Margaret Landis,[§] George Lem,[||] Ben O'Shaughnessy,*,[⊥] and Nicholas J. Turro[‡]

Department of Chemistry, Columbia University, New York, New York 10027;
Central Research Division, Pfizer Inc., Eastern Point Road, Groton, Connecticut 06340;
Firmenich Chemical Manufacturing Center, 150 Firmenich Way, Port Newark, New Jersey 07114; and
Department of Chemical Engineering, Columbia University, New York, New York 10027

ABSTRACT: We present the first ever measurements of living chain molecular weight distributions (MWDs), $\psi^o(N)$, in free radical polymerization (FRP), using a new technique, the "photocopy method". Though living chains are the fundamental objects in FRP, their MWDs have eluded measurement until now, principally due to their very short lifetimes ($\lesssim 1$ s). In the photocopy method, the living population is converted, essentially instantaneously, to a labeled inert one by "photoinhibitor" molecules activated by a short laser pulse. This floods the FRP with photoinhibitor radicals, which ideally (i) are extremely slow to initiate new living chains yet (ii) couple with existing living chains (and each other) at near diffusion-controlled rates and (iii) carry a fluorescent label. Thus, the living chains are "frozen" and labeled. They are subsequently detected selectively using GPC equipped with a fluorescence detector (a second detector simultaneously detects unlabeled chains). We applied the photocopy method to low conversion methyl methacrylate FRP. Our measured MWDs are exponential as predicted by the classical Flory−Schulz theory (which ignores the chain length dependence of the termination rate constant, k_t), but only for chains longer than the mean living chain length $\bar{N}_o$. For $N < \bar{N}_o$, our data are consistent with a stretched exponential as predicted by modern FRP theories accounting for N dependence of k_t. However, the small N data may also be accounted for by nonideal effects, initiation of new living chains by photoinhibitors, which lead to power law behavior. Another complication is that thermal initiation persists during the photocopying process in its present form. Thus, post-laser-pulse initiated living chains react with photoinhibitor radicals, distorting the measured MWDs from that of the steady-state living chains. From the measured living and dead MWDs, we infer living and dead chain concentrations and mean lengths and the fraction of living chains terminating via coupling. Finally, using reported values of propagation rate constants, we estimate mean living chain lifetime, polymerization rate, and the average termination rate constant.

I. Introduction

Free radical polymerization (FRP) is of tremendous technological importance, as a significant portion of the approximately 70 billion pounds of plastic and other polymeric materials produced annually in the U.S. is made by some form of FRP.[1,2] Consequently, intense research efforts have focused in understanding the mechanisms underlying FRP since its early developments in the 1930s.[3−16] Despite this, many fundamental issues in FRP remain poorly understood today. Most notably it remains a subject of controversy as to what mechanisms underlie the "gel effect"[3] of FRP, during which polymerization rates "autoaccelerate" and molecular weights of dead chains being produced are observed to increase by up to an order of magnitude.[1,3,17]

In FRP, the most crucial properties to measure are those of the propagating radicals, i.e., "living chains", which are the loci of polymerization events. The dynamics of this living chain population determine all other FRP properties and thus are the natural focus of theory and experiment. The living population is a highly reactive nonequilibrium object with a typical lifetime of a few seconds or less. It is for this reason that measurements of living chain properties are scarce. In particular, measurements of living chain molecular weight distributions (MWDs) have been lacking. Here, we present a novel, "photocopying" method to measure living chain MWDs for the first time ever.[18] The living MWD contains a wealth of information: (i) it reflects statics and dynamics of living chains and provides the most direct test of FRP theories, and (ii) it allows extraction of essentially all relevant FRP parameters. For these reasons, measurements of the living MWDs are extremely desirable from both a fundamental and a technological point of view. In this article, we report the first ever measurements of living chain MWDs, obtained using the photocopying method in the polymerization of methyl methacrylate (MMA) at low conversion ($\lesssim 1\%$). Our measured living MWDs agree with the exponential distributions predicted by Flory and Schulz *only for chains longer than a certain length*. For shorter chains, we find substantial deviations from the simple Flory−Schulz prediction. Although these are not inconsistent with modern theories of FRP[19] which take into account the chain length dependence of the termination rate constant between living chains, we cannot exclude the possibility that these deviations originate from side reactions affecting our results for the short chain distribution. Actually, the novel method we devised allows the *simultaneous* measurement of both the living MWD and the dead MWD derived from it. This allows

* To whom correspondence should be addressed. E-mail: bo8@columbia.edu.
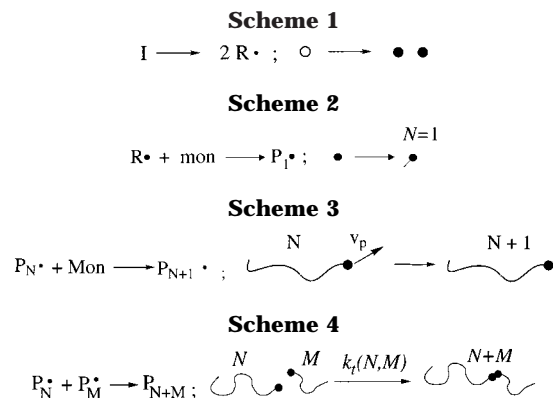† Present address: Institut Curie, Section de Recherche, Laboratoire PCC, UMR 168, 11, rue Pierre et Marie Curie, 75231 Paris Cedex 05, France.
‡ Department of Chemistry, Columbia University.
§ Pfizer Inc.
|| Firmenich Chemical Manufacturing Center.
⊥ Department of Chemical Engineering, Columbia University.

Scheme 1

$$I \longrightarrow 2\,R\cdot \;;\; \circ \longrightarrow \bullet\,\bullet$$

Scheme 2

$$R\bullet + mon \longrightarrow P_1\bullet \;;\; \bullet \longrightarrow \overset{N=1}{\bullet}$$

Scheme 3

$$P_N\cdot + Mon \longrightarrow P_{N+1}\cdot \;;$$

Scheme 4

$$P_N^\bullet + P_M^\bullet \longrightarrow P_{N+M} \;;$$

us to check whether the living population, currently impossible to obtain by other methods, is consistent with the dead one. Using the measured living and dead MWDs, we access directly, from a single experiment, a large number of FRP parameters, some of which are difficult to obtain by existing methods.

The experiments reported in this article concern "bulk" FRP, producing linear chains, where the monomer itself acts as the solvent. This is the simplest possible FRP system, where the reaction vessel initially contains[3] almost pure unsaturated monomer, e.g. MMA. Small amounts of "initiator" are also present, typically organic azo or peroxide compounds which decompose spontaneously at a certain rate to produce free radicals (Scheme 1). Each freshly generated radical attacks a monomer (Scheme 2), attaching itself and transferring its live radical center to the monomer. A growing living chain, or macroradical, is produced as successive monomers are added in similar fashion, at "velocity" v_p monomers per second (Scheme 3). Living chains propagate into the surrounding monomer solution. In many cases, chain growth is terminated by an interpolymeric reaction in which a pair of living chains annihilate one another's radical end groups via coupling (Scheme 4). The result is a "dead" polymer chain; this is the final polymer product. The termination step may result in two dead chains rather than one; these so-called disproportionation events (section V.E, Figure 11) do not affect the kinetics of FRP, nor the properties of the living population, but modify the MWD of the dead polymer product. For a FRP at steady state, from its "birth" until its "death" a living chain lives, on average, a time $\tau_{living}^0 \equiv \bar{N}_0/v_p \lesssim 1$ s, where $\bar{N}_0$ is the mean steady state living chain length. In addition to initiation, propagation and termination, another fundamental process takes place in FRP, namely chain transfer,[3,1] in which an initiator radical or a growing living chain loses its active center to another species, typically to the monomer solvent. This produces one dead chain and a fresh living chain. Since the chain transfer rate of PMMA living chains to MMA monomer is very small,[3,1,20] this process is neglected here.

Under typical conditions,[1,3] the living chain population rapidly ($\lesssim 1$ s) reaches a steady state in which macroradical creation and termination rates balance. As the polymerization runs its course, more and more dead chains accumulate, and the conversion ϕ (the fraction of monomer initially present converted to polymer) gradually increases on a time scale *much longer* (minutes or hours) than the time scales characterizing the living chain kinetics (seconds or less): to a good approximation, living chain kinetics occur in a
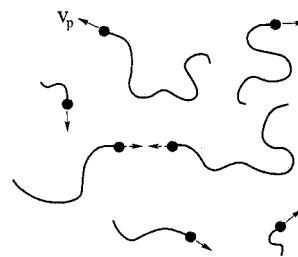

Figure 1. Schematic of a FRP mixture. Shaded background represents dead chains and monomer: at conversion ϕ, this is a dead polymer solution at polymer volume fraction ϕ. Living chains (foreground) are (i) growing at rate v_p monomer/s (proportional to propagation rate constant k_p) and (ii) involved in interpolymeric reations which terminate growth, converting them to dead chains.

fixed environment.[3] The properties of this environment, primarily consisting of dead chains plus monomer solvent, are changing quasi-statically. At any instant, the reaction mixture contains a population of growing living chains with a *broad distribution of lengths*. This living population is very dilute in a dead polymer solution (of volume fraction nearly equal to the conversion ϕ), in a solvent of unreacted monomer (Figure 1). We note that MMA is a good solvent for its polymer PMMA.

The essence of the novel photocopy method presented here is to convert the highly reactive and short-lived living chain population into a labeled dead one which is thereafter analyzed using standard methods. This is achieved by flooding the polymerization with small "photoinhibitor" radicals, generated by a laser flash. These radicals are very slow in initiating new living chains but couple with existing ones (and one another) at near diffusion-controlled rates. Furthermore, the photoinhibitor radicals carry a fluorescent label. The effect is to freeze growth of the living chain population and to simultaneously produce a labeled dead copy of it.

Our starting point for the selection of a suitable photoinhibitor molecule is the work of Guillet and co-workers,[21−26] who introduced the concept of "phototerminators" and with these attempted to control kinetics of FRP. Another major interest was to produce fluorescently labeled polymers.[26,25] Holdcroft and Guillet[22] initiated polymerizations by photolyzing the initiator 2,2-′azobis(isobutyronitrile) (AIBN) using laser pulses of one wavelength, and terminated them by photolyzing the phototerminator 2-naphthylmethyl 1-naphthyl acetate (NMNA) using a second laser pulse at a different wavelength. They used styrene as the monomer both in solutions and in microemulsions. Later, they extended their studies to methyl methacrylate (MMA) polymerizations.[24] However, they encountered serious difficulties due to side reactions. Peak molecular weights in styrene polymerizations were observed to be 111 000 in the absence of phototerminator, whereas in the presence of phototerminator it was 9200, indicating that NMNA interfered with the FRP. Using moderate laser intensities (≈ 5 mJ/pulse/cm^2) they discovered that labeled chains actually contained many (up to 100) labels per chain. Reducing the laser intensity by a factor of 10 resulted in one or less labels per chain to be produced. Guillet and co-workers typically used thousands of laser shots in their experiments, partly due to the low efficiency[21] (quantum yield $\approx 6\%$) of the pho-

toterminator NMNA to produce radicals upon photolysis. Later, Guillet and co-workers shifted their focus from the study of FRP to producing fluorescently labeled polymers. They developed photochemical "iniferters" which produce, upon photolysis, a radical which is reactive toward monomer and another which is not. The more reactive radical initiates polymerization, while the other one kills growing chains, labeling them at one end.[25,26] Our experiments are very much inspired and informed by the work of the Guillet group. However, our primary interest is to develop a general method to study basic mechanisms in FRP by measuring living chain molecular weight distributions (MWDs).

In the next section, we briefly review both classical and modern theoretical predictions for steady state living chain MWDs. In section III, we describe the novel photocopying method, while in section IV, we present our measurements of MWDs of living chains at steady state. These distributions are compared with classical predictions of Flory and Schulz[3] and with recent FRP theories.[27] We also consider side reactions likely to perturb our measurements. We then show in section V how one can calculate a large number of important FRP parameters, such as living chain concentrations, from the MWDs. It is also indicated that by measuring non-steady state properties of living chains one can obtain dynamical parameters such as steady state mean living chain lifetimes, τ^o_{living}, and propagation velocities, v_p, directly using the photocopy method. Both of these issues are dealt with in detail in the accompanying article.[28] Section VI is where we discuss our results, while section VII is concerned with experimental details.

II. Flory−Schulz Theory and Beyond

In this section we briefly discuss living MWDs as predicted by the classical Flory−Schulz theory, and by recent theories of FRP. The simple and elegant theory developed by Flory[3] and Schulz and Husemann[29] in the 1930s has remained the reference point in experimental and theoretical investigations of FRP. The basis of this theory is the assumption that termination rate constants k_t (and the propagation rate constants k_p) are *independent* of living chain lengths and dead chain concentration. Flory theory has been very successful in predicting kinetics of FRP at high dilution[3] ("low conversion"), although there is convincing experimental evidence[9−11,30−32] that, even at low conversions k_t depends on chain length. We will see below how the predictions of the Flory−Schulz theory are modified[27] when one considers the dependence of k_t on chain length at low conversions. At higher conversions, the Flory approximation becomes completely inadequate[33−35] as dead polymer accumulates in the polymerization mixture, slowing down the dynamics of reacting chains, and causing the famous autoacceleration phenomenon.[1]

According to theory, the success of the Flory theory during *low* conversion FRP stems from a weak power law dependence of termination rate constant on chain lengths at low polymer concentrations. Systematic renormalization group theoretical calculations[19] of polymer−polymer reaction rate constants, as well as physically motivated scaling theories, are consistent with photophysical measurements of phosphorescence quenching rates between end labeled polymers[32,36−38] which indicate a weak dependence of k_t on chain length. That is, theory and experiments indicate that, for reacting

chains of the same length, N, k_t has the following form:

$$k_t \sim \frac{1}{N^\alpha} \tag{1}$$

Different values of the exponent α are predicted, depending on whether excluded volume interactions[39] dominate living chain dynamics ($\alpha \approx 0.16$, ref 19), which requires rather long chains, or Rouse dynamics[39] are dominant ($\alpha = 1/2$, ref 40). In model experiments using phosphorescence quenching mentioned above $\alpha \cong 0.2−0.3$ are found. The essential point is that the chain length dependence of k_t at low conversions is "weak", i.e., $\alpha < 1$.

The second crucial point for understanding the living MWD is the "short wins" principle, for reactions between chains of different lengths. Theory predicts,[41] with some experimental support,[42−44] that k_t is dominated by the *shorter* chain, i.e., $k_t(N, M) \approx k_t(N)$ for $N \ll M$.

Now, to obtain the steady-state living MWD, let us consider the dynamics of living chains, which obey:[9,34,35]

$$\frac{\partial \psi}{\partial t} = -v_p \frac{\partial \psi}{\partial N} - H\psi, \; \psi(0) = \frac{R_i}{v_p} \tag{2}$$

where $\psi(N, t)$ is the number of living chains of length N units at time t, and $H(N, t)$ is the "reaction field", i.e., the total reaction rate per chain of length N due to all other living chains in the system, given by

$$H(N, t) \equiv \int_0^\infty dM \, k_t(N, M)\psi(M, t) \tag{3}$$

The formal solution of eq 2 at steady state is

$$\psi^o(N) = \psi^o(0) \, \exp\left(-\frac{1}{v_p}\int_0^N H \, dN\right) \tag{4}$$

from which it is clear that the living MWD is determined by the reaction field which, in turn, is determined by the form of k_t.

Flory−Schulz Theory:[3] The reaction field within the context of Flory theory (eq 3 with $k_t = $ cste) is simply the inverse of the mean radical lifetime: $H_{Flory} = k_t\psi^o_1 = 1/\tau_{living}$, which is independent of chain length, and where $\psi^o_1 \equiv \int_0^\infty \psi^o \, dN$ is the total number density of living chains. From eq 4, this immediately implies an exponential distribution for the living chains at steady state: $\psi^o(N) \sim e^{-N/\bar{N}_o}$.

Chain Length Dependent k_t:[27] Now we take into account the chain length dependence of k_t (eq 1 with $\alpha < 1$), following the theory of O'Shaughnessy in ref 27, and consider the reaction field acting on long and short chains, respectively:

(i) Long chains ($N \gg \bar{N}_o$): The reaction field is now $H(N) \equiv \int_0^\infty dM \, k_t(N, M)\psi^o(M) \approx \int_0^\infty dM \, k_t(M)\psi^o(M) = $ cste, where we have used the "small wins" principle. Since $H(N)$ is independent of chain length, the living chain distribution at steady state is exponential, from eq 4: $\psi^o(N)e^{-B(N/\bar{N}_o)}$ where B is a constant.

(ii) Short chains ($N \ll \bar{N}_o$): The reaction field acting on short chains is $H(N) \equiv \int_0^\infty dM \, k_t(N, M)\psi^o(M) \approx k_t(N) \psi^o_1$, where we again made use of the "small wins" principle. Using this expression for H and $k_t(N)$ from eq 1 in eq 4, we see that the living MWD for short chains is a stretched exponential: $\psi^o(N) \sim \exp(-C[N/\bar{N}_o]^{1-\alpha})$, with C being a constant.
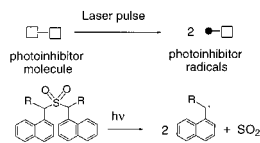
Figure 2. Top: a photoinhibitor molecule, which does not interfere with the FRP, photolyzed by a laser pulse to produce "photoinhibitor radicals" which do not attack monomer at substantial rates, are highly reactive toward any radical, and carry a label. Bottom: arylmethyl sulfone compounds, such as DNS (R ≡ −H) and DNPMS (R ≡ −Ph) which come close to being ideal photoinhibitors.

In summary, modern FRP theories[27] predict the following steady-state living chain MWD at low conversions:

$$\psi^0(N) \sim \begin{cases} e^{-C(N/\bar{N}_o)^{1-\alpha}}, & N \ll \bar{N}_o \\ e^{-BN/\bar{N}_o}, & N \gg \bar{N}_o \end{cases}, \text{ theory} \qquad (5)$$

where B and C are constants. The numerical value of the exponent α depends on the living chain environment, i.e., on dead chain concentration and solvent quality. Usually, as for the PMMA polymerizations here, the unpolymerized monomer is a good solvent for the chains. That is, excluded volume effects are important. In this case, theory predicts[19] $\alpha \approx 0.16$. However, it is established experimentally that universal excluded volume exponents require rather large N values; for shorter chains, we may expect Zimm or even Rouse dynamics to apply,[39] leading to different α values. Finally, for chains so short (typically a few tens of units) as to be less than the polymer persistence length, the very concept of α breaks down. We will see below that our experimental measurements of the living MWD are consistent with a form as in eq 5. However, we will also see that it is difficult to extract a precise experimental value for the exponent α from our data and, furthermore, that we are unable to exclude the presence of side reactions which may be interfering with our measurements, at least for shorter chains.

III. Photocopy Experiment

In the novel photocopying method the short-lived living chains are converted to a *labeled* dead population by use of "photoinhibitor molecules" which cleave to yield, with high efficiency, "photoinhibitor radicals" when photolyzed at an appropriate wavelength (Figure 2). Photoinhibitor molecules do not interfere with polymerization until they are converted to photoinhibitor radicals. In the *ideal case*, these radicals possess the following very special properties which are crucial for the success of the method:

1. They do not attack the monomer, that is, they do not initiate new living chains. Clearly, any addition to monomer would create labeled chains which would make an unwanted contribution to the measured labeled dead MWD.

2. They are highly reactive toward living chains (and one another), coupling with them at near diffusion-controlled rates. At sufficiently high photoinhibitor radical concentrations, this allows intercepting the growth of essentially all living chains.

3. They carry a label which can be selectively detected with high sensitivity. Thus, by coupling with living chains, they create labeled dead chains which can be distinguished from the unlabeled ones.
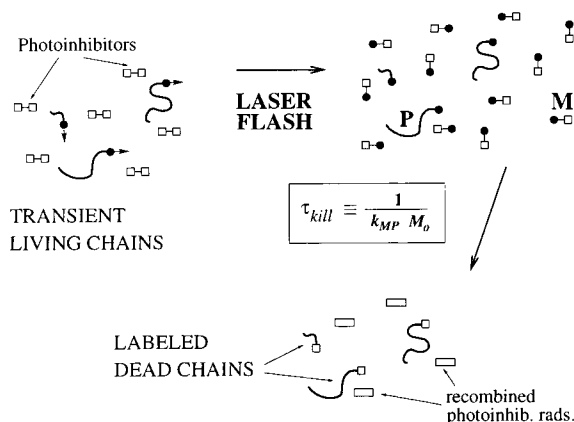

Figure 3. Reaction where a laser pulse floods a steady state FRP with special photinhibitor radicals (see Figure 2) which then kill and label living chains, converting them to *labeled* dead chains. Actually, most of the photoinhibitor radicals recombine with one another due to their much higher concentration compared to that of the living chains. Ideal photoinhibitor radicals do not initiate new living chains. The labeled dead chain population is a good copy of the transient living chains which existed just before the laser flash, provided the photocopy process takes a time τ_{kill} much shorter than the mean living chain lifetime in steady state, τ^0_{living}; i.e. $\tau_{\text{kill}} \ll \tau^0_{\text{living}}$ (see text).

Some radicals stabilized by aromatic structures, such as derivatives of the naphthylmethyl radical (Figure 2), come close to satisfying all these requirements.[21−24,45] In particular, we have found that the photoinhibitor molecule di(1-naphthyl, phenyl methyl) sulfone (DNPMS, Figure 2) comes closest to satisfy the conditions cited above among a number of molecules tested.[18]

The photocopy experiment is carried out as follows. Photoinhibitor molecules are included in the initial FRP mixture in addition to monomer and small amounts of thermal initiator which are present as in standard FRP. As the temperature of the mixture is raised to a sufficient level (typically 50−90 °C), the initiator molecules start decomposing and the polymerization begins. Following thermal equilibration, the FRP quickly (typically seconds) reaches a steady state in which living chains are being created and destroyed (producing dead chains) at equal rates. During these stages, the photoinhibitor molecules do not interfere with the polymerization; i.e., they are inert. However, at a given moment in the polymerization, a very short laser pulse creates a large concentration of "photoinhibitor radicals" from the photoinhibitor molecules, as shown in Figure 3. The laser pulse duration ($\cong$ 20 ns) is much faster than $1/\nu_p$, the time it takes to add one monomer to a growing living chain (typically[31,20] $10^{-3}-10^{-4}$ s). That is, the photoinhibitor radicals are created essentially instantaneously. Because of their special properties, these radicals do not initiate new living chains yet couple with existing ones (and one another) at near diffusion-controlled rates. Thanks to the label they carry, the living population they kill becomes a *labeled* dead population, which can be distinguished from the unlabeled dead chains (Figure 3). We note that since the photoinhibitor radicals flood the system, in fact most of them recombine with one another, producing products which typically differ from the starting photoinhibitor molecule, as a SO₂ group is lost in the process (Figure 2). The recombined photoinhibitor radical products do not interfere with the measurement of labeled dead chains, provided they are well separated in weight from the high molecular weight
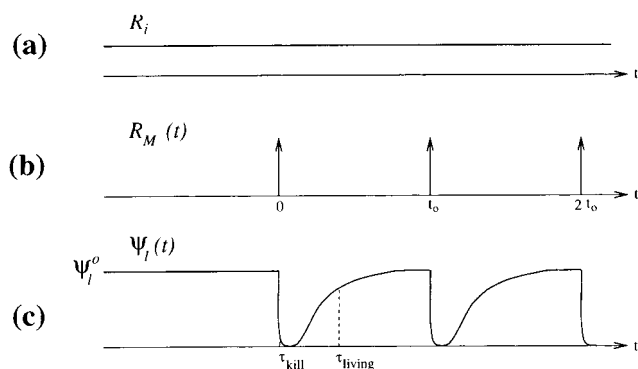
(a)

(b)

(c)

Figure 4. Schematic timing diagram for the photocopy experiment. Fresh living chains are created at a constant rate R_i by the decomposition of a thermal initiator (a). The rate R_M at which photoinhibitor radicals are created is a series of δ-pulses (b), since these radicals are generated "instantly" using very short laser pulses. The effect on the living chain concentration ψ_1^o is dramatic (c). Living chains are killed (and labeled) with each laser pulse on a time scale tkill, then recover their steady state concentration ψ_1^o on a much longer time scale, of order τ_{living}^o. The process is repeated with period t_o, much longer than τ_{living}^o, to accumulate identical copies of the steady state living chain population.

polymer by gel permeation chromatography[46](GPC) prior to detection, as will be discussed shortly.

Since the concentration of photoinhibitor radicals just following a laser pulse, M_o, is much higher than the concentration of living chains at steady state, ψ_1^o, a given living chain almost certainly will react with a photoinhibitor radical, rather than with another living chain. Thus, the time scale for killing living chains is determined by the photoinhibitor radical (M)−living chain (P) coupling rate constant, k_{MP}, and the initial photoinhibitor radical concentration M_o: $\tau_{kill} \equiv 1/(k_{MP}M_o)$. Since the concentration M_o can be readily manipulated, e.g., by varying the laser intensity, the time scale τ_{kill} can be made much shorter than the mean living chain lifetime, $\tau_{living}^o = \bar{N}_o/v_p \cong 0.1−1$ s. When this condition is satisfied, living chains will be killed by photoinhibitor radicals before they have had a chance to grow substantially. That is, the labeled dead population will be a *good copy of the living population* that existed just before the laser pulse.

Note that the thermal initiation rate, R_i, is unchanged during this process. Thus, fresh living chains continue to be produced during and following the photocopying process, and the living chain population recovers steady state on a time scale of the order of the mean living chain lifetime τ_{living}^o, much longer than τ_{kill}, as illustrated schematically in Figure 4. Thereafter, the photocopying process can be repeated in order to accumulate labeled dead copies of the living chains. Provided the laser period is sufficiently long so that steady state is recovered between pulses, identical copies of the steady-state living chain population will be accumulated (see the accompanying article[28] for more details on the effect of varying the laser period). This improves signals from the labeled chains when they are analyzed later.

The photolyzed sample which contains the labeled copy of the living population is analyzed using GPC, which separates molecules according to their hydrodynamic sizes. In this technique, elution times increase with decreasing molecular weights. Our GPC instrument is equipped with two detectors in series as shown
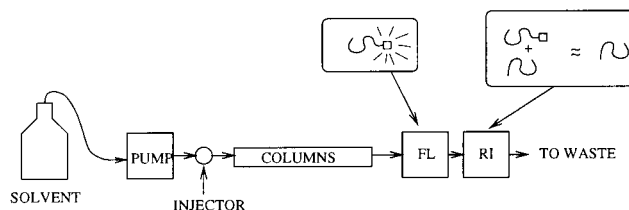

Figure 5. Following photolysis, analysis of the mixture containing labeled and unlabeled dead chains using GPC equipped with two detectors. The excitation and emission wavelengths on the fluorescence detector (FL) are set such that only the labels contribute to observed signals. The refractive index (RI) detector does not distinguish labeled chains from unlabeled ones. When most of the chains are unlabeled, the RI detector essentially measures the dead population.

in Figure 5. One of these is a fluorescence (FL) detector in which the excitation and emission wavelengths are set such that only the fluorescent labels contribute to observed signals. That is, *the FL detector observes only the labeled dead copy of the living population* which existed just before the photocopying laser pulse. Note that the small molecular weight recombination products of photoinhibitor radicals (or other potentially fluorescent small compounds) result in a very high amplitude peak at the total inclusion limit[46] (largest elution times) of the chromatograms, but this should not interfere with the measurement of the labeled living population beyond a certain threshold due to the chromatographic separation of sizes prior to detection.

The second detector is a refractive index (RI) detector which does not distinguish labeled chains from unlabeled ones. In the experiments, the dead chains are allowed to accumulate in the solution for a few minutes as the FRP runs its course before the photocopying pulses are applied. Thus, after the living chain population is copied to a labeled dead one a few times over, most of the polymer in the solution still consists of unlabeled chains. Under these conditions, *the RI detector essentially measures only the dead population.* Thus, in summary, in the photocopy experiment both living and dead MWDs can be measured *simultaneously.* However, for accurate measurements of the dead MWD, care must be taken to allow for a long enough thermal FRP prior to photocopying laser shots. This is because, in experiments where the thermal FRP prior to laser shots is kept very short (≲2−3 min), the measurement of the dead population will be more sensitive to perturbations caused by the induction period and by nonsteady-state periods due to the photoinhibiting laser pulses.

Possible Complications. Before ending this section, let us consider potential complications due to (i) propagation of living chains during photocopying, (ii) initiation (by thermal decomposition of the initiator AIBN) persisting during the photocopying process, and (iii) photoinhibitor radicals having a finite rate of addition to monomer. We will discuss these points in the context of the Flory−Schulz theory (k_t independent of chain length), and for (i) and (ii) assuming that the photoinhibitor radicals behave *ideally* (their rate of addition to monomer is zero). We use roman scripts (P, M, etc.) to refer to species, and italics (*P*, *M*, etc.) to refer to concentrations of these species.

(i) Chain Growth during Photocopying. Living chain growth during the photocopying process can be ignored if the photocopying is sufficiently fast, such that the living chains are killed well before they can grow a

length comparable to the mean living chain length $\bar{N}_o$ = $v_p\tau_{living}^o$, where v_p is the propagation velocity, and τ_{living}^o is the mean lifetime of living chains at steady state. That is, the extent to which the living chains grow during the photocopying process, $\delta N \equiv v_p\tau_{kill}$ should be small compared to $\bar{N}_o$: $\delta N \ll \bar{N}_o$. It follows that propagation effects will be small if $\tau_{kill} \ll \tau_{living}^o$. This condition is automatically satisfied when the FRP system is flooded with photoinhibitor radicals, i.e., $r \equiv \psi_1^o/M_o \ll$ 1. This follows from the expressions for $\tau_{living} = 1/k_t\psi_1^o$ and $\tau_{kill} = 1/k_{MP}M_o$, with the photoinhibitor radical (M)—living chain (P) coupling rate constant, k_{MP}, being the same order of magnitude as the living chain (P)—living chain (P) termination rate constant: $k_{MP} = \mathcal{O}(k_t)$.

(ii) Post-Laser-Flash Initiation. Since initiation of living chains (from the decomposition of thermal initiator) persists during the photocopying process, some post-laser-flash generated living chains will react with photoinhibitor radicals, creating labeled dead chains which distort the measured MWD from that of the steady-state living chains. The amount of distortion caused up to time τ_{kill} following a laser flash will be small, since the amount of post flash generated living chains (at rate R_i), $\psi_1^{\tau_{kill}} = R_i\tau_{kill}$, will be small compared to the steady-state concentration of living chains which are being measured, $\psi_1^o = R_i\tau_{living}^o$, provided $\tau_{kill} \ll \tau_{living}^o$. Thus, at time τ_{kill} essentially all living chains which existed before the laser flash will have been killed and a very small amount of living chains will have been generated by thermal initiation. On the other hand, the concentration of photoinhibitor radicals will have dropped only by a factor of unity from its initial value, M_o, and hence, $M(\tau_{kill}) \gg \psi_1(\tau_{kill})$, where ψ_1 is the concentration of living chains. These photoinhibitor radicals will survive[47] up to times of order τ_{living}^o and be available for reactions with post-laser-flash generated living chains. The amount of labeled dead chains produced by such reactions will be of the order $R_i\tau_{living}^o = \psi_1^o$; i.e., comparable to the steady-state living chain concentration the experiment aims to measure. The distortion of the measured MWDs will be biased toward small chains ($N < \bar{N}_o$); in particular, the MWD of labeled dead chains produced by this process is predicted[47] to diverge weakly for short chains ($N \ll \bar{N}_o$): $\psi_d \sim \ln(\bar{N}/N)$. This is not inconsistent with our measured labeled dead chain distributions (Figure 8). A complete analysis of thermal initiation effects will be presented in a future article.[47]

The problems due to initiation being kept on during photocopying will be completely eliminated in future experiments, using photoinitiators (which can be excited selectively compared to the photoinhibitor molecules). Using photoinitiators the rate of initiation, R_i, can be modulated at will; thus continuous photoinitiation (R_i = cste) can be turned off ($R_i = 0$) just before the moment a photoinhibition pulse is applied. Such an experiment is described in the accompanying article.[28]

(iii) Nonideal Photoinhibitors. In practice, the photoinhibitor radicals will have a finite rate of addition to monomer ("initiation" of living chains by DNPMS derived radicals); that is, they will be nonideal. The effects of having a finite addition rate are analyzed theoretically in refs 18, 28, and 47. The analysis indicates that addition has a small effect on the measured MWDs, provided the addition time scale, τ_{add}, is much longer than the mean living chain lifetime, τ_{living}^o. However, if this condition is not satisfied, a significant

portion of the initial photoinhibitor radicals may add to monomer, creating unintentionally labeled chains (which have nothing to do with the living chains of steady state FRP), and would thereafter be detected along with the intentionally labeled chains, marring our living chain measurements. Thus, it is important to know how the measured distributions would be affected if this "pollution" process is significant. In ref 47, the dead MWD resulting from the "pure" pollution process (where the only source of living chains is due to addition of photoinhibitor radicals to monomer, i.e., there is no thermal initiation) is calculated. For this case, a $1/N$ distribution is predicted for pollutant dead chains which are shorter than a certain length $N^* \equiv v_p\tau_{add}$, where $\tau_{add} \equiv k_{add}$ [mon] is the time required for a photoinhibitor radical to add to monomer, with k_{add} being the photoinhibitor radical addition rate constant to monomer and [mon] the monomer concentration. Some control experiments, testing the addition of photoinhibitor radical to monomer, are presented in the accompanying article.[28]

We will see shortly that this $1/N$ distribution due to the pure pollution process is actually rather close to our experimental measurements for chains shorter than the mean living chain length. However, for these same chains, our experimental results are also consistent with the stretched exponential dependence predicted (eq 5) in the complete absence of pollution! Thus, in the accompanying article[28] we attempt to quantify by other means whether, in practice, addition of photoinhibitor radicals to monomer is relevant by a number of experiments. The results of these experiments, albeit indirect, suggest that pollution should have a small effect when the photoinhibitor DNPMS is used.

IV. Results. Living Chain Molecular Weight Distributions

In a typical experiment, 147 mg (9.0×10^{-3} M) of the initiator AIBN and 20 mg (4.1×10^{-4} M) of the photoinhibitor DNPMS are dissolved in 100 mL neat MMA monomer. With these concentrations, the absorption of the laser light at 308 nm is negligible for the initiator AIBN and the monomer (see section VII). A 200 μL aliquot of the DNPMS/AIBN/MMA mixture is placed in a rectangular clear fused quartz cell with a 0.3 cm path length, and argon gas is bubbled through the solution for $\approx$ 5 min to remove oxygen which acts as an inhibitor for FRP. Following degassing, the sealed cell is placed in a thermostat as shown in Figure 6 at 60 °C. At this temperature, and at the concentration used, the initiator AIBN decomposes to provide a rate of initiation $R_i \cong 10^{-7}$ M/s (section VII). The sample is allowed to polymerize thermally for 2−4 min before 5−10 laser shots at 308 nm are applied with a period t_o $\geq$ 10 s, much longer than the mean living chain lifetime at steady state, τ_{living}^o. The laser beam is expanded using a divergent lens in order to excite the whole sample. The variation in laser light intensity throughout the sample volume is estimated to be less than a factor of 3. Immediately following photolysis, the sample is removed from the thermostat, and 100 μL of the mixture is diluted with 400 μL THF. This diluted mixture is allowed to relax for at least 20 min before it is injected into the GPC (Figure 5), equipped with a fluorescence (FL) and a refractive index (RI) detector. The excitation (300 nm) and emission (350 nm) wavelengths on the FL detector are set such that only the naphthalene derivative labels contribute to the observed signals. On the
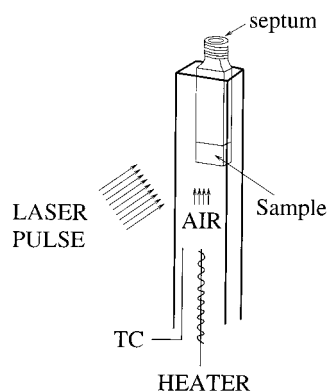
Figure 6. Photolysis setup for the photocopy experiment. Temperature control is maintained via hot air flowing through a clear fused quartz tube. A temperature controller regulates the heater current, based on feedback from a thermocouple (TC) placed near the sample position. The sample is polymerized thermally for 2–4 min before 5–10 laser pulses are applied. The laser beam is expanded using a divergent lens (not shown) to excite the whole sample.
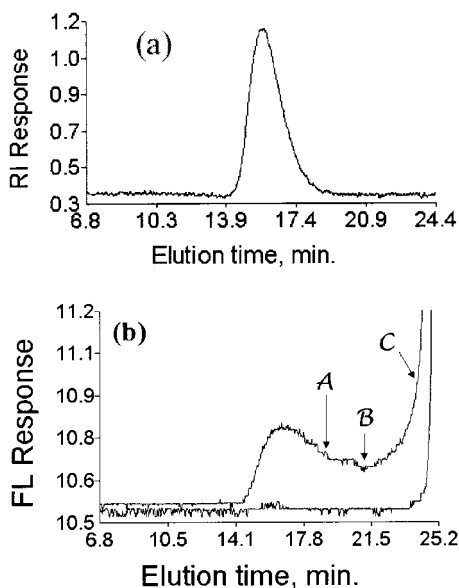

Figure 7. (a) Typical GPC chromatogram obtained in the photocopy experiment (see text) for the DNPMS/AIBN/MMA system using the refractive index (RI) detector. (b) Top chromatogram of the same sample as in part a, but obtained using the fluorescence (FL) detector. Different low MW (high elution time) limits of integration that are used in calculating $\bar{N}_0$ and $\psi_1{}^0$ are indicated: $\mathcal{A}$, $t \cong 19.0$ min (MW $\cong$ 27 000); $\mathcal{B}$, $t \cong 21.1$ min (MW $\cong$ 5000); $\mathcal{C}$, $t \cong 24.1$ min (MW $\cong$ 600). The chromatogram at the bottom, slightly offset vertically for clarity, is from a DNPMS/AIBN/MMA sample which is subjected only to the thermal FRP part of the experiment (no laser shots).

other hand, the RI detector is sensitive to any polymer that passes through its detection cell, whether labeled or not. Typical RI and FL chromatograms obtained this way are shown in Figure 7. Some differences between the two chromatograms immediately draw attention. First, the FL chromatogram is significantly shifted toward longer elution times, that is toward lower molecular weights (MWs), as compared to the RI chromatogram. This shift is not due to the time required for the solution to flow from one detector to another, as in fact, the solution first passes through the FL detector. Rather, the shift is due to the following factors:

1. A labeled chain contributes one unit to the FL signal, independent of its length. In contrast, a chain contributes to the RI detector signal an amount that is proportional to its own length. That is, the FL signals are biased toward the number-average molecular weight (MW), M_n, while the RI signals are biased toward the weight-average MW, M_w. With these very polydisperse samples, the difference between the two MW averages can be considerable ($M_w/M_n \approx 2-3$). We note that if many labels were being put randomly on living and dead chains, as Guillet and co-workers had encountered during their studies with other photoinhibitors,[21-26] the FL signals would be "mass based" as the RI signals are, and consequently the two chromatograms would appear similar.

2. Part of the dead chains are generated via the coupling of living chains (section V.E, Figure 11). This means that the mean dead chain length, $\bar{N}_d$, is actually longer than the mean living chain length, $\bar{N}_0$ (in the extreme case of termination via only coupling,[3] $\bar{N}_d = 2\bar{N}_0$). This issue is discussed in more detail later in section V.E.

It should be added that termination of post-flash thermally generated living chains with photoinhibitor radicals, and addition of photoinhibitor radicals to monomer would both distort the measured FL chromatograms from those expected from properly killed and labeled steady-state living chains.

Another point in Figure 7 worth noting is the intensities of the RI and FL signals. Although the living chains measured in this experiment using the FL detector have a concentration that is several orders of magnitude smaller than that of the dead chains which accumulate for a few minutes during the thermal FRP that precedes the photolysis of the sample, the FL signals have a quite acceptable signal-to-noise ratio. This, of course, is due to the much more sensitive nature of the FL detection.

Finally, the FL chromatogram in Figure 7 includes a very large amount of small MW polymer at high elution times. At the highest elution times (beyond $\cong$23 min) part of a very large peak, due to small molecular weight compounds (due to recombined photoinhibitor radicals—MW = 434.58—, and/or intact photoinhibitor—MW = 498.64) can be seen. The tail of this large peak (toward smaller elution times, or higher MWs) is presumably interfering to some degree with the measurement of the much smaller peak due to labeled dead chains (peaked around 17 min). However, it is difficult to explain the presence of substantial amount of signals at high elution times (between about 17 and 21 min) simply as being due to interference from the adjacent small MW peak. One reason is that the range of MW between these elution times is quite large (from MW $\cong$ 4000 to 100 000, see section VII.C). In addition, attempts to better separate the two peaks by adding an extra column with very high resolution in the relevant MW range results in similar chromatograms: the signals never reach baseline level between the two peaks. Finally, a large peak is present in DNPMS/AIBN/MMA samples which are not photolyzed, but with its tail starting to be distinguishable from the baseline only beyond 24 min, as shown in Figure 7b. The intensity of this large peak actually increases as more photoinhibitor is photolyzed, since the recombination products of photoinhibitor radicals (lacking the SO_2 moiety) are more highly fluorescent than the precursors. That is, after photolysis, interference from the small MW peak should be more significant. Nonetheless, these considerations suggest that the effect seen cannot be merely explained by
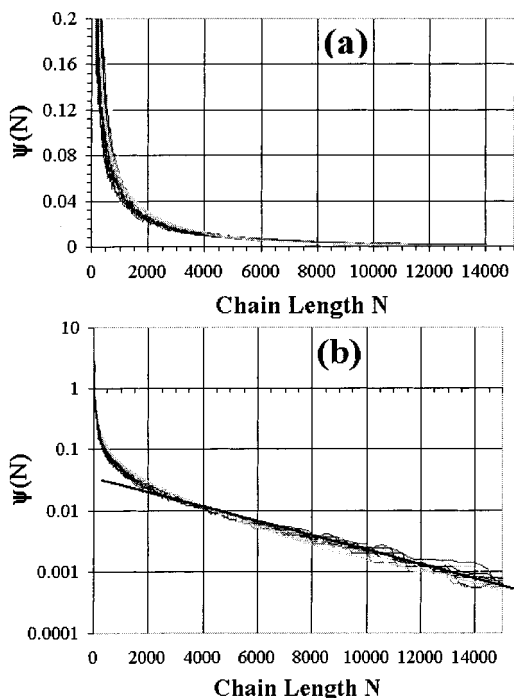
Figure 8. (a) Living MWD plotted on linear coordinates for the DNPMS/AIBN/MMA system for 11 samples, measured under comparable conditions. The MWDs are vertically shifted to compensate for their different normalizations. (b) MWDs in part a plotted on a semi-logarithmic scale. The straight line, a linear regression for chain lengths 3000 < N < 16 000, has slope $-(2.8 \pm 0.4) \times 10^{-4}$.

the high MW tail of the larger peak interfering with the measurement of the smaller one: there must be a large amount of oligomeric labeled chains produced in these experiments.

From the FL chromatogram in Figure 7 the MWD is calculated using the MW calibration of the FL detector (section VII.C). In the calculation, the fact that the FL detector is sensitive to the number density of labeled chains is taken into account. The resulting *living MWD* is plotted in Figure 8 in both linear and semilogarithmic coordinates, along with 10 other measurements, obtained under similar conditions. A linear regression to the $N = 3000$ to $N = 16\,000$ region on the semilogarithmic plots in Figure 8b gives $\psi^o(N) = ((3.14 \pm 0.33) \times 10^{-2}) \times \exp[(-2.8 \pm 0.4) \times 10^{-4}N]$, with a regression coefficient higher than 0.99. Thus, the MWD obeys an exponential distribution for chains longer than a certain length $\bar{N} \cong 2{-}3000$ (or MW $\cong 2{-}300\,000$, since the monomer has MW $\cong 100$). We will see in section V.A that the length scale $\bar{N}$ separating the exponential, long chain part and the nonexponential, short chain parts of the measured distributions is very close to the mean living chain length, $\bar{N}_o$.

The distribution followed by shorter chains, $N \ll \bar{N}$, on the other hand, deviates strongly from the Flory–Schulz prediction. The deviation is actually in very good accord with the predictions of modern FRP theories (section II, eq 5), as can be seen in Figure 9, where a function of the form $c_1 \exp(-[N/c_2]^{1-\alpha})$ is fit to the data for the region 40 < N < 1500, using $\alpha = 0.2$ and $\alpha = 0.5$. Notice that the agreement (using either value of α) improves as one moves toward shorter chains, as predicted by theory. We observe from Figure 9 that using $\alpha = 0.5$ for the fits results in slightly better agreement with the data than using $\alpha = 0.2$. This result
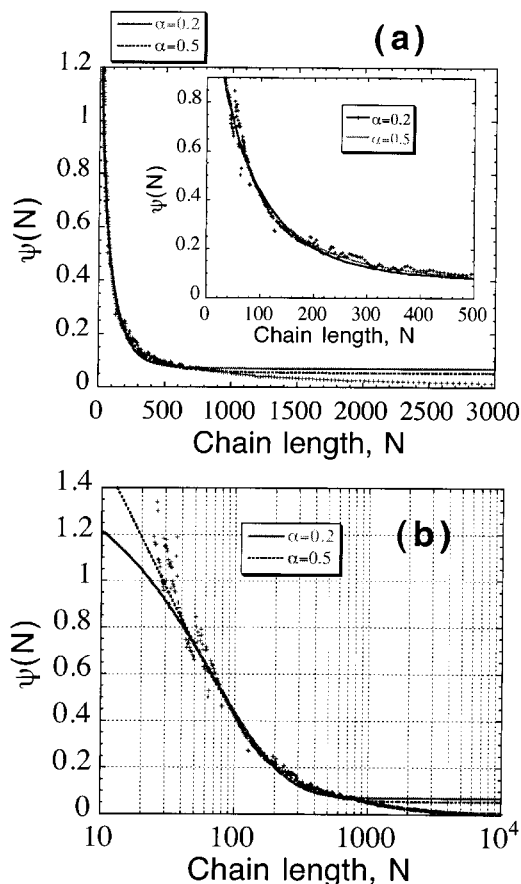

Figure 9. (a) Short chain part of a representative living MWD measurement (+ signs) for th DNPMS/AIBN/MMA system from Figure 8. Least squares fits of the data for the region 40 < N < 1500 to a function of the form $c_1 \exp(-[N/c_2]^{1-\alpha})$ are also shown, with values of α as indicated ($c_2 \cong 68$ and $c_2 \cong 24$ when $\alpha = 0.2$ and $\alpha = 0.5$ are used, respectively). The inset shows a zoom to smaller scales. (b) Experimental data (+ signs) and the same fits as in part a, plotted on a logarithmic–linear scale.
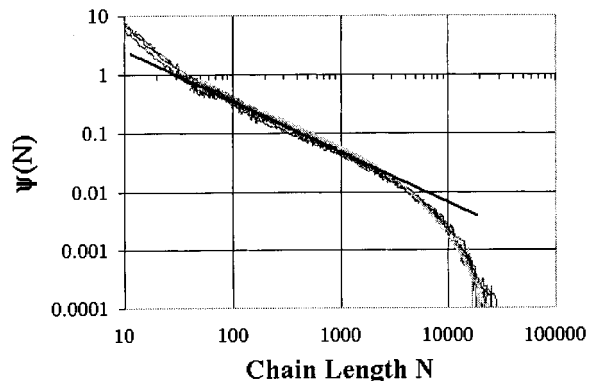

Figure 10. Short chain portions of the 11 living MWDs of Figure 8. plotted on double logarithmic coordinates. The straight line, a linear regression for chain lengths 40 < N < 2000, has slope -0.884 ± 0.026.

suggests that Rouse dynamics[39] may describe the behavior of these chains.

Now, although our measurements may be in accord with modern FRP theoretical predictions of eq 5, a closer look reveals that our short chain data can also be described rather well by a power law: $\psi^o \sim N^{-\gamma}$ (Figure 10). Recall that such a power law, with $\gamma = 1$, is predicted for the pure pollution process for chains shorter than a certain threshold $N^* = v_p \tau_{add}$ (section III)

Table 1. Quantities Measured in the Photocopy Experiment (Second Column, Using Photoinhibitor DNPMS) and Comparison with Independent Estimates or Measurements (Third Column), or Reported Values (Fourth Column), for the FRP of MMA at 60 °C, Initiated with 9×10^{-3} M AIBN ($R_i \cong 10^{-7}$ M/s)

	photocopy	indep. est.	lit.
$\psi^o(N)$	$\sim \begin{cases} e^{-a_1(N/\bar{N}_o)^{1-a}}, & N \ll \tilde{N} \\ e^{-a_2 N/\bar{N}_o}, & N \gg \tilde{N} \end{cases}$		
	$\alpha \cong 0.2-0.5^l$		
	$a_2 = 0.59 \pm 0.04$		
	$\tilde{N} = 2-3000$		
$\bar{N}_o$	2100 ± 100	2800^a $\bar{N}_d/2 \leq \bar{N}_o \leq \bar{N}_d$	m
ψ_1^o (M)	$(2-3) \times 10^{-7}$	$4 \times 10^{-8\,b}$	$\leq 10^{-7\,c}$
v_p (s^{-1})			6930^d
τ_{living}^o (s)	0.3^e	0.4^f	varies
$\bar{N}_{dead}$	3300 ± 200	$\bar{N}_o \leq \bar{N}_d \leq 2\bar{N}_o$	varies
R_p (M/s)	$(1-2) \times 10^{-3\,g}$	$2.8 \times 10^{-4\,h}$	varies
k_t (M^{-1} s^{-1})	$1 \times 10^{7\,i}$	$6 \times 10^{7\,j}$	$10^6-10^{8\,k}$
f_d	0.43		0.46^k

^{a} From $\bar{N}_o = R_p/R_i$, with calculated R_i from known rate of decomposition of AIBN and independently measured R_p. ^{b} From $\psi_1^o = R_p/v_p$, with R_p from independent measurements, v_p from ref 53, for pure MMA. ^{c} Typical values. ^{d} From ref 53, for pure MMA. ^{e} From $\tau_{living}^o = \bar{N}_o/v_p$, with $\bar{N}_o$ from photocopy experiment, v_p from ref 53, for pure MMA. ^{f} From $\tau_{living}^o = \bar{N}_o/v_p$, with $\bar{N}_o$ from footnote a, v_p from ref 53, for pure MMA. ^{g} From $R_p = v_p\psi_1^o$, with ψ_1^o from the photocopy experiment, v_p from ref 53, for pure MMA. ^{h} Measured from slope of ϕ vs polymerization time data. ϕ from GPC, RI detection. ^{i} From $k_t = 1/(\tau_{living}^o\psi_1^o)$, with τ_{living}^o and ψ_1^o from photocopy expt. ^{j} From $k_t = 1/(\tau_{living}^o\psi_1^o)$, with τ_{living}^o from footnote f, ψ_1^o from footnote b. ^{k} Values reported in the *Polymer Handbook*[20] for FRP of MMA at 60 °C. ^{l} Slightly better agreement with larger values of α. $a_1 \approx 15.5$ (9.2) for $a = 0.2$ (0.5). Data for $N \ll \tilde{N}$ is also well described by $\psi^o \sim N^{-\gamma}$, with $\gamma = 0.88 \pm 0.03$. ^{m} We are not aware of any previous *direct* measurements of $\bar{N}_o$.

wherein photoinhibitor radicals behave nonideally and add to monomer, creating new, unwanted living chains. Thus, it is important to verify the value of the exponent γ and try to quantify the influence of photoinhibitor radical addition to monomer in our measurements. The short chain data (for the same 11 measurements shown in Figure 8) are thus replotted in Figure 10, on double logarithmic coordinates. A linear regression for chain lengths $N = 40$ to $N = 2000$ on this plot yields $\gamma = 0.884 \pm 0.026$, with regression coefficient higher than 0.99. The MWDs in Figures 8 and 10 are shifted vertically in order to account for their different normalizations (due to differences in the number of laser shots used). Although the measured exponent γ is certainly less than unity, the value predicted for pure pollution, it is not far off from it, and the complex nature of the pollution process[47] does not allow us to draw any conclusions with confidence. On the other hand, the following considerations suggest that the pollution process may not be important in our living MWD measurements:

• The crossover length $\tilde{N}$ separating the exponential and the nonexponential regimes in the measured MWDs is very close to the mean living chain length, $\bar{N}_o = v_p \tau_{living}^o$ (section V.A), suggesting that the origin of the two different regimes is physical and has to do with living chain dynamics. However, it is possible that pollution is present and $\bar{N}_o \approx N^*$, where $N^* = v_p\tau_{add}$ is the crossover chain length predicted[47] for the pure pollution process (section III). We note that if $\tau_{add} \ll \tau_{living}^o$ were true, then most of the labeled dead chains would be produced via pollution,[47] with a characteristic length $N^* \ll \bar{N}_d$, which is inconsistent with our measurements (see below).

• The slopes of the short chain MWDs on the log–log plot of Figure 10 are independent of the laser intensity employed, hence of the concentration M_0 of photoinhibitor radicals produced per laser pulse. The MWDs plotted on Figure 10 were obtained using laser intensities varying by more than a factor of 6. If the addition of photoinhibitor radicals to monomer were significant, then we would expect the slope to tend to -1 as the laser intensity is increased, which would render the pollution process more severe.

• All the FRP parameters we measure are consistent with one another and agree fairly well with independent estimates and values available in the literature, as summarized in Table 1.

• A rather subtle point, discussed in the accompanying article,[28] is that the total number of labeled chains we measure saturates as the concentration M_0 of the photoinhibitor radicals produced per laser pulse is increased (via increasing the photocopying laser intensity). If a significant fraction of the photoinhibitor radicals were to add to monomer, then increasing M_0 would result in a corresponding increase in the total amount of labeled chains detected. However, in ref 47 it is shown, for the pure pollution process, that this increase is a slowly increasing logarithm of M_0 above a certain threshold value, which may be consistent with our measurements. The initial increase in the total amount of labeled polymer is explained by an increasing fraction of labeled chains being killed and labeled by photoinhibitor radicals as the concentration of these latter is increased.

Some of these points are discussed in more detail in the accompanying article.[28] The possibility that pollution may be important in our measurements is weakened by these considerations, which, however, are all based on indirect evidence. Hence our results, at least for short chains, should be taken with some caution. Another reason to take our data with some caution is due to the process of post-flash thermally generated living chains reacting with photoinhibitor radicals which survive up to times of order τ_{living}^o.

To summarize, our data is well described by

$$\psi^o(N) \sim \begin{cases} e^{-a_1(N/\bar{N}_o)^{1-\alpha}}, & N \ll \tilde{N} \\ e^{-a_2 N/\bar{N}_o}, & N \gg \tilde{N} \end{cases} \quad \text{(experiment)} \quad (6)$$

where the short chain exponent $\alpha \cong 0.2-0.5$ (with somewhat better agreement using higher values of α), $a_1 \approx 15.5$ ($a_1 \approx 9.2$) for $\alpha = 0.2$ ($\alpha = 0.5$), $a_2 = (0.588 \pm 0.04)$ and the cross over length $\tilde{N} \cong 2000-3000$. Equation 6 represents *the first ever measurements of living chain distributions in FRP*. These results are also shown in Table 1, in the second column where quantities measured in the photocopy experiment are summarized.

In the following section, we calculate a number of important FRP parameters, using the living chain distributions presented in this section. The large number of such parameters demonstrates the power of the photocopy method. Furthermore, these parameters can be compared with one another for internal consistency, can be checked against existing measurements and against independent estimates. These comparisons provide challenging tests for the validity of the photocopy technique.

V. FRP Parameters from Living MWDs

A. Mean Living Chain Lengths. With the living and dead chain MWDs at hand, it is possible to calculate

a number of important parameters. Starting with the living MWD, $\psi^o(N)$, two important parameters that can readily be accessed are the mean living chain length, $\bar{N}_o \equiv [\int_0^\infty N\psi^o(N)\,dN]/[\int_0^\infty \psi^o(N)\,dN]$, and the total living chain concentration, $\psi_1^o \equiv \int_0^\infty \psi^o(N)\,dN$.

Now, to calculate mean living chain lengths, $\bar{N}_o$, and total living chain concentrations, ψ_1^o, one needs to integrate the FL chromatogram in Figure 7b. However, because the response never drops back to baseline level at the low MW end (large elution times) before interference with small MW compounds starts, setting this low MW integration limit is somewhat arbitrary and subject to errors. In repeated experiments, we have found that the minimum $\mathscr{B}$ marked on Figure 7b consistently appears at about 21 min (MW $\cong$ 4000−5000) and is insensitive to variations in external parameters such as the laser power, or the laser period. Thus, point $\mathscr{B}$ seems to be a convenient and reasonable limit to use. We will see below, and in the accompanying article that the choice of limit $\mathscr{B}$ gives results that are consistent with a number of independent estimates for $\bar{N}_o$. In all values reported below for $\bar{N}_o$ and ψ_1^o, $\mathscr{B}$ is used as the low MW limit of integration, unless stated otherwise.

To determine how sensitive our results are to the choice of the low MW integration limit, we compared limit $\mathscr{B}$ to additional limits, marked $\mathscr{A}$ and $\mathscr{C}$ in Figure 7b. Limit $\mathscr{A}$ is at 19.0 min elution time, corresponding to MW $\cong$ 27 000, obviously a choice that is too high. On the other hand, limit $\mathscr{C}$ is at 24.1 min (MW $\cong$ 600), possibly containing some interference from the adjacent large peak to the right. Results using limit $\mathscr{A}$ will be biased toward high MWs, while the ones using limit $\mathscr{C}$ will be biased toward low MWs. Notice that the errors due to the choice of the cutoff will be more important for measurements of *absolute* quantities than *relative* ones.

For the chromatogram shown in Figure 7b, using limit $\mathscr{B}$, the mean living chain length $\bar{N}_o$ is calculated to be $\cong$ 2140 (or the number-average MW $M_n^{\text{living}} \cong$ 214 000) and the polydispersity ($M_w^{\text{living}}/M_n^{\text{living}}$) $\cong$ 3.0. In comparison, we find $\bar{N}_o \cong$ 3070 ($M_n^{\text{living}} \cong$ 307 000) when limit $\mathscr{A}$ is used, and $\bar{N}_o \cong$ 1,510 ($M_n^{\text{living}} \cong$ 151 000) when limit $\mathscr{C}$ is used.

Averaging results over seven experimental runs, and using cutoff $\mathscr{B}$, we obtain $\bar{N}_o \approx$ 2100, with a standard deviation of 100, as shown in the second column in Table 1. This directly measured value of $\bar{N}_o$ can be checked against an independent estimate of the mean living chain length, obtained via the relation $\bar{N}_o = R_p/R_i$, where the rate of polymerization, R_p, is measured independently (see section V.F), and the rate of initiation is calculated from the known decomposition rate of the initiator AIBN (section VII). This yields $\bar{N}_o = (2.8 \times 10^{-4}$ M/s)/(10^{-7} M/s) = 2800 as shown in the third column of Table 1. This independent estimate of $\bar{N}_o$, which may be sensitive to uncertainties in the efficiency factor used in estimating the rate of initiation, R_i, is nevertheless in close agreement with the directly measured value reported above.

B. Concentration of Living Chains, ψ_1^o. In the past, electron paramagnetic resonance (EPR) has been the only generally applicable method in measuring living chain concentrations in FRP.[48,49] However, for many species, including MMA, due to the low concentration of living chains it is very difficult to obtain acceptable EPR signals at low conversions.[49,48] Some

measurements could only be made using specially built high sensitivity EPR cavities,[50] or cells[51] which nevertheless required signal averaging during which time significant conversion (up to 20%) took place.

Fluorescence, on the other hand, is a much more sensitive technique[52] to measure concentrations, provided molecules with high absorptivity and fluorescence yields are used. The fluorescent labels used in the photocopy experiment, naphthalene derivatives, are excellent fluorophores:[52] our GPC fluorescence detector is capable of easily detecting concentrations of the model compound 1-methylnaphthalene as low as 10^{-8} M, using typical instrumental settings (see section VII.C). Calibration of the GPC FL detector for the concentration of this compound, a model for the labels derived from DNS in the photocopy experiment, is shown in Figure 13.

When DNPMS is used in the photocopy experiment, the labels that result are somewhat different than 1-methylnaphthalene, and a better model compound for calibration of FL detector signal intensities is 1-benzyl-naphthalene. The fluorescence yield of 1-benzylnaphthalene is about 6.5% higher than that of 1-methyl-naphthalene at the excitation (λ_{ex} = 300 nm) and emission (λ_{em} = 350 nm) wavelengths employed in the analysis. Using the calibration in Figure 13, and appropriately correcting for the higher fluorescence yield of 1-benzylnaphthalene, we can estimate the concentration of living chains measured in the photocopy experiment. For the DNPMS/AIBN/MMA system, typical concentrations calculated this way are $\psi_1^o \cong$ (2−3) $\times$ 10^{-7} M, as shown in the second column of Table 1.

Since the rate of polymerization, R_p, is the product of the propagation velocity, v_p, and the living chain concentration, ψ_1^o, measuring R_p separately and using reported values of v_p provides an independent estimate of the living chain concentration that can be compared to the directly measured values reported above. The propagation velocity, $v_p = k_p[\text{mon}]$, where k_p is the propagation rate constant and [mon] is the monomer concentration, is best measured using the pulsed laser polymerization (PLP) technique. Using k_p = 770 M^{-1} s^{-1} for bulk MMA polymerization at 60 °C, reported in ref 53, the concentration of neat MMA, [mon] = 9 M, and separately measured rate of polymerization (section V.F), we calculate $\psi_1^o = R_p/v_p \cong$ (2.8 $\times$ 10^{-4} M/s)/(6930/s) $\cong$ 4 $\times$ 10^{-8} M. This value, shown also in the third column in Table 1, is 5−7 times lower than the values calculated directly from the FL chromatograms above. Possible reasons for the disagreement are errors involved in the measurement of the rate of polymerization, in setting the integration limits for the FL chromatograms (see above), and errors stemming from the concentration calibration of the FL detector. In particular, the fluorescence yield of the polymer bound labels may be different than that of the model compounds used for the concentration calibration of the FL detector. However, this difference in fluorescence yields is expected to be small, since it is known that fluorescence yields of alkyl substituted naphthalenes do not vary significantly with the size of the alkyl groups.[54] Other sources of error are post-flash generated living chains reacting with photoinhibitor radicals and possibly the pollution process.[28,47]

C. Living Chain Lifetime τ_{living}^o, and Termination Rate Constant, k_t. Mean living chain lifetimes, τ_{living}^o, can be estimated from the measured living chain lengths (section V.A) and the propagation velocity from

ref 53 we used above: $\tau_{\text{living}}^o = \bar{N}_o/v_p = 2100/(6930\ \text{s}^{-1})$ $\cong 0.3$ s. Using this value, an average termination rate constant for living chains, $k_t = 1/(\tau_{\text{living}}^o\ \psi_l^o) \cong (1.1-1.7)$ $\times 10^7\ \text{M}^{-1}\ \text{s}^{-1}$ is readily obtained, which falls within the broad range of values reported in the *Polymer Handbook*.[20] The results for τ_{living}^o and k_t are shown in the second column of Table 1.

The mean living chain lifetime can also be obtained using our previous independent estimate for $\bar{N}_o$ (Table 1, third column) and the propagation velocity from ref 53: $\tau_{\text{living}}^o = 2800/(6930\ \text{s}^{-1}) \cong 0.4$ s, as shown in the third column of Table 1. With this value of the mean living chain lifetime and the living chain concentration ψ_l^o estimated independently (see above and third column in Table 1), we obtain $k_t = 1/[(0.4\ \text{s})(4 \times 10^{-8}\ \text{M})]$ $\cong 6 \times 10^7\ \text{M}^{-1}\ \text{s}^{-1}$. This estimate of the termination rate constant, also within the range of values reported in the *Polymer Handbook*,[20] is entered in the third column in Table 1.

Since the propagation velocity is not measured in experiments probing steady state properties of living chains reported in this article, values of τ_{living}^o and k_t reported here are based on published values of the propagation rate constant v_p. In the accompanying article,[28] we demonstrate how v_p and τ_{living}^o can be directly measured in photocopy experiments probing *non-steady state* properties of living chains.

D. Mean Dead Chain Lengths and Dead Chain Concentrations. The mean dead chain length, $\bar{N}_d$, is calculated from the RI chromatogram in Figure 7a to be approximately 3510 (or $M_n^{\text{dead}} \cong 351\ 000$), and the polydispersity (PD) of the dead population $M_w^{\text{dead}}/M_n^{\text{dead}}$ $\cong 2.0$. Averaging results over seven experimental runs, we find $\bar{N}_d \cong 3300 \pm 200$ (second column, Table 1). We note that the mean living chain lengths, $\bar{N}_o$, calculated above using three different integration limits, all fall approximately within $\bar{N}_d$ and $\bar{N}_d/2$, as required if the experiment indeed measures the living MWD (see below). This requirement is also indicated in the third column of Table 1.

One of the great advantages of simultaneously measuring both the dead and the living MWDs is that it allows us to see how the living MWD is mapped into the dead one. The same living MWD, in fact, can produce different dead MWDs depending on the mode of termination and the importance of chain transfer. When a significant fraction of living chains terminate through coupling, for example, it is predicted[3] that the resulting dead MWD is much sharper than the original living one. This prediction by Schulz,[3] made in 1939, is confirmed directly by our measurements for the first time. Compared to the polydispersities obtained above for the living MWD (PD $_{\text{living}} \cong 3.0$), we observe that the dead MWD is indeed much sharper (PD$_{\text{dead}} \cong 2.0$). We will see in the next section how the mode of termination can be determined using the photocopy method, and that indeed an important fraction of the living chains do terminate via coupling.

Before ending this section, we note that in experiments where the thermal FRP prior to laser shots is kept very short ($\lesssim 2-3$ min), the measurement of the dead population will be more sensitive to perturbations caused by the induction period and by non-steady-state periods due to the photoinhibiting laser pulses. Thus, whenever we compared dead MWDs to living ones, we used longer polymerization times.[55]
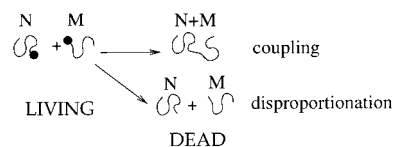
Figure 11. Possible termination mechanisms in FRP, between two chains of lengths N and M. A third mechanism, namely chain transfer, which results in one dead and one freshly generated ($N = 1$) living chain, is negligible[20] for MMA.

E. Mode of Termination. The simultaneous measurement of both living and dead chain distributions and consequently the corresponding mean chain lengths in the photocopy experiment allows us to determine the mode of termination, as follows. The termination mechanism in FRP involves either coupling or disproportionation as shown in Figure 11. In the extreme case of 100% coupling, the mean dead chain length is twice the mean living chain length,[3,35] $\bar{N}_d = 2\bar{N}_o$, while in the other extreme (100% disproportionation), the two means are equal, $\bar{N}_d = \bar{N}_o$, assuming $k_t =$ cste. Thus, in the general case where a fraction f_d of living chains terminate via disproportionation, one can write the following equation:

$$\bar{N}_d = f_d\bar{N}_o + (1 - f_d)2\bar{N}_o \qquad (7)$$

Therefore, in the photocopy experiment it is, in principle, possible to infer the relative roles of coupling vs disproportionation in termination events, since the dead and living populations are measured simultaneously.

Solving eq 7 for f_d and using $\bar{N}_o = 2100$ (section V.A) and $\bar{N}_d = 3300$ (section V.D) obtained above, we find $f_d = 2 - (\bar{N}_d/\bar{N}_o) \cong 0.43$ (second column in Table 1), in excellent agreement with the value reported in the *Polymer Handbook*[56] for FRP of MMA at 60 °C ($f_d = 0.46$, fourth column in Table 1). This latter value should be taken with some caution, however, as "there remains considerable uncertainty in existing termination mode measurements and there is wide variation in results for common monomers such as styrene and methyl methacrylate"[57] as reviewed and discussed by Zammit et al.[57] and by Solomon and Moad.[16]

We remind the reader that the calculation of $\bar{N}_o$ is sensitive to the integration limits set on the FL chromatograms. Since the MWD contains a large amount of small molecular weight polymer, setting the lower integration limit is subject to errors. Nevertheless, the fact that $\bar{N}_o$ is always within $\bar{N}_d$ and $\bar{N}_d/2$ for any choice of cutoff between the high ($\mathscr{A}$) and low ($\mathscr{O}$) values is reassuring.

F. Rate of Polymerization. Using reliable propagation velocities reported in the literature,[53] and the living chain concentration ψ_l^o measured directly by the photocopy technique (section V.B), we can estimate the rate of polymerization, $R_p = v_p\psi_l^o$. Thus, we obtain $R_p = 6930\ \text{s}^{-1} \times (2-3) \times 10^{-7}\ \text{M} = (1-2) \times 10^{-3}$ M/s, as indicated in the second column in Table 1.

On the other hand, measuring the rate of polymerization in a separate experiment allows comparison with the polymerization rate obtained above from the photocopy experiment. This also allows us to obtain independent estimates for the living chain concentration $\psi_l^o = R_p/v_p$ and the mean living chain length $\bar{N}_o = R_p/R_i$, and thus to check whether the photocopy method gives results that are consistent with these independent
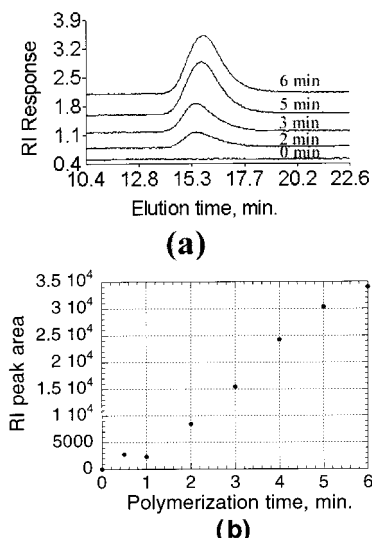
(a)

(b)

Figure 12. (a) GPC chromatograms obtained with the RI detector as a function of the thermal polymerization times indicated. (b) Integrated peak areas of the chromatograms in (a), plotted as a function of thermal polymerization time for methylmethacrylate at 60 °C. Initiator (AIBN) concentration is 9×10^{-3} M. The solution also includes 5.8×10^{-4} M DNS.

estimates. In addition, the polymerization kinetics and dead chain distributions obtained in the presence and absence of photoinhibitors are compared to see whether the photoinhibitor molecules are really inert during the thermal polymerization part of the photocopy experiment. Finally, measuring the rate of polymerization independently helps in quantifying the concentration regimes explored in our experiments. This latter point is important, as the termination rate constant is known to be a weak function of chain length only at sufficiently low conversions.

Similar thermal polymerization kinetics are observed using a number of different photoinhibitors of the type shown in Figure 2. For example, thermal polymerization kinetics of the DNS/AIBN/MMA mixture, followed using the RI detector of the GPC equipment, is shown in Figure 12a, where the photoinhibitor DNS is dinaphthyl sulfone (Figure 2). Defining time zero as the moment the sample is placed in the thermostat at 60 °C, a plot of the integrated RI peak areas as a function of polymerization time is shown in Figure 12b. A short, reproducible induction period of 0.5−1 min is observed. A linear increase in RI response follows the induction period for the polymerization times investigated. Using the calibration of the RI detector for PMMA concentration (section VII.C, Figure 14), the information in Figure 12 can be used to calculate a rate of polymerization, R_p, of about 2.8×10^{-4} M/s (third column, Table 1). Using the photoinhibitor DNPMS results in similar polymerization kinetics.

As an indication that the photoinhibitor does not interfere with the thermal polymerization part of the photocopy experiment, similar (within 20−30%) polymerization rates, average MWs, and polydispersities are observed for thermal FRPs (no laser shots) in the absence and presence of DNPMS, keeping everything else constant. Finally, using the initiator lauroyl peroxide (LPO, Fluka Chemika) instead of AIBN, we found similar RI and FL chromatograms. In these experiments, the concentration of LPO is 5.6×10^{-3} M, giving a rate of initiation $R_i \approx 10^{-7}$ M/s, the same as in the case of AIBN.

Finally, we quantify the conversion regimes in which our results have been obtained. Typically, total FRP times are kept below 4−5 min, including the period when laser shots are applied. The volume fraction of dead polymer accumulated at the end of 5 min thermal FRP (uninterrupted with laser pulses) is $\phi(t = 5 \text{ min}) \cong 0.4\%$. Thus, typical total conversions should be lower when laser shots, which interrupt the polymerization, are used. Though this conversion value is very small, it is still somewhat higher than the overlap threshold,[39] $\phi^* = 1/(\bar{N}_d)^{-4/5} \cong 0.2\%$ for the typical MWs produced in our experiments, $\bar{N}_d \cong 3000$. Thus, even with the very short polymerization times and the low rate of initiation that are employed, we are probing the regime near $\phi \approx \phi^*$. Though ideally we would like to explore more dilute regimes ($\phi \ll \phi^*$), the chain length dependence of the termination rate constants[58] should still be of the type $k_t \sim 1/N^\alpha$ with $\alpha < 1$ for the conversion regimes explored here.[32,58−60]

VI. Discussion

In this article we presented a novel experimental technique, the "photocopy method", which allows measurements of the molecular weight distribution of living chains in FRP. Although we presented results for bulk FRP, with appropriate modifications, it may be possible to apply the photocopy method to some of the more complex FRP systems, e.g., solution or microemulsion polymerizations.

Although the living distribution is a fundamental quantity in FRP, its measurement has defied conventional techniques in more than 6 decades of research, mainly due to the highly transient and reactive nature of the living chains, and their small concentrations. Measuring the living chain population itself, rather than some indirect quantity derived from it offers tremendous advantages.

The basic idea behind the use of "photoinhibitor" molecules goes back to Guillet and co-workers[21−26] whose primary interest was to control kinetics of FRP and to produce fluorescently labeled polymers. Our primary interest, however, is to develop a general analytical method to study basic mechanisms in FRP by measuring living chain MWDs.

Our living chain measurements suggest (eq 6) (i) an exponential distribution, $e^{-a_2 N/\bar{N}_o}$, for long chains ($N \gg \tilde{N}$) and (ii) a stretched exponential distribution, $\exp(-a_1(N/\bar{N}_o)^{1-\alpha})$, for short chains ($N \ll \tilde{N}$), where the crossover length $\tilde{N} \cong 2000−3000$ is indistinguishable from the mean living chain length $\bar{N}_o \cong 2100 \pm 100$. These measurements appear to be inconsistent with the classical Flory−Schulz theory[3] which ignores the chain length dependence of the termination rate constant k_t. They are consistent, however, with recent FRP theories[27] accounting for chain length dependence of k_t. Two essential ingredients of the theory are the "short wins" principle ($k_t(N, M) \approx k_t(N)$ for $N \ll M$), and the weak dependence of k_t on chain length; $k_t \sim 1/N^\alpha$ with $\alpha < 1$, for $N = M$. We compared two values of the exponent α: $\alpha = 0.2$, which is close to the theoretically predicted[19] $\alpha = 0.16$ when excluded volume interactions dominate living chain dynamics, and $\alpha = 1/2$, appropriate for Rouse dynamics.[40] Satisfactory agreement was obtained in both cases with our data, although the agreement is slightly better when the latter value for α is used. These conclusions, we stress again, are somewhat tentative given the possibility of MWD distortion through the

pollution process (see below) and distortion due to thermal initiation persisting during the photocopying process.

We noted that the short chain ($N \ll \tilde{N}$) portion of the MWDs can also be well described by a power law, $\psi^o(N) \sim N^{-\gamma}$, with an exponent $\gamma = 0.88 \pm 0.03$. Such a distribution is not inconsistent with some fraction of photoinhibitor radicals adding to monomer and hence creating new, unintentionally labeled chains which are later detected along with the intentionally labeled ones. In the case where there are only photoinhibitor-radical-initiated living chains ("pure pollution"), a $1/N$ law is predicted[47] for the dead MWD, for chains shorter than a certain length $N^* = v_p \tau_{add}$, where τ_{add} is the time it takes a photoinhibitor to add to monomer. Assuming that the origin of the measured power law is indeed the addition side reaction, we identify $N^* = \tilde{N} \cong 2000-3000$, leading to the estimate $\tau_{add} = \tilde{N}^*/v_p \cong 0.3-0.4s$. Since the cross over length $\tilde{N}$ is very close to the mean living chain length $\bar{N}_0$, the time scale τ_{add} calculated above is consequently very close to the mean living chain lifetime, $\tau^0_{living} \cong 0.1-1$ s. Such a value for the addition time scale τ_{add} is too long to be measured directly by conventional spectroscopic techniques (such as laser flash photolysis[18,61−63]) since radical−radical recombination events provide a much faster pathway to the disappearance of photoinhibitor radicals than addition to monomer, even at very low concentrations of radicals and in neat monomer. However, it is short enough to perturb the measurements of living chain MWDs.[28,18,47]

The following considerations, on the other hand, go against the idea that the addition of photoinhibitor radicals to monomer is relevant, as discussed in section IV. (i) The crossover length, $\tilde{N}$, separating the two regimes in eq 6 is very close to the mean living chain length, $\tilde{N}_0$, suggesting that the origin of the two different regimes has to do with FRP living chain dynamics and is not due to an artifact (unless, of course $\tau_{add} \approx \tau^0_{living}$—see above); (ii) the slopes of the short chain MWDs on the log−log plot of Figure 10 are independent of the laser intensity employed, hence of the concentration M_0 of photoinhibitor radicals produced per laser pulse; (iii) as discussed in ref 28, the total number of labeled chains measured saturates as the concentration M_0 of the photoinhibitor radicals produced per laser pulse is increased; (iv) the FRP parameters measured using the photocopy method are, overall, consistent with one another and agree fairly well with the independent estimates and values available in the literature, as summarized in Table 1. Since all of these considerations are based on indirect evidence, the possibility of addition side reaction influencing our measurements, though rendered weaker, cannot be excluded.

A serious complication arises from the rate of initiation, R_i, being kept constant during the photocopying process. Following a photoinhibition pulse essentially all living chains which existed just before the laser pulse are killed and labeled on a time scale $\tau_{kill} \ll \tau^0_{living}$. Meanwhile, fresh living chains are generated at rate R_i from the decomposition of the thermal initiator, AIBN. These chains are also killed and labeled by photoinhibitor radicals, creating labeled dead chains which distort the measured MWD from that of the steady-state living chains. The amount of post-flash generated chains up to time τ_{kill}, $\psi_1^{\tau_{kill}} = R_i \tau_{kill}$, is small compared to the steady-state concentration of living chains which are being measured, $\psi_1^o = R_i \tau^0_{living}$, provided $\tau_{kill} \ll \tau^0_{living}$.

However, many photoinhibitor radicals will survive past τ_{kill} and continue to react with post-flash generated living chains until the photoinhibitor radical concentration becomes small compared to that of living chains, which will take a time[47] $t^* \approx \tau^0_{living}$. The amount of labeled dead chains produced during this period will be of order $R_i \tau^0_{living} = \psi_1^o$, i.e., comparable to the steady-state concentration of living chains. The distortion of the measured MWDs caused by this process will be biased toward small molecular weights; in particular, a weak (logarithmic) divergence for short chains ($N \ll \bar{N}_0$) is predicted, which is not inconsistent with our data. In future experiments we are planning to eliminate this unwanted thermal initiation effect using photoinitiators, which can be excited selectively compared to the photoinhibitor molecules. This way continuous photoinitiation can be turned off (R_i set to zero) just before a photoinhibition pulse is applied. Such an experiment is described in the accompanying article.[28]

Our experiments have provided *the first ever measurements of living chain distributions in FRP*. Aside from their significance for the fundamental understanding of FRP, these distributions allow a large number of FRP parameters to be readily obtained. From the steady state distribution, mean chain lengths, $\bar{N}_0$, and total living chain concentrations, ψ_1^o, are calculated. Using reliably measured propagation velocities reported in the literature, mean steady state living chain lifetimes $\tau^0_{living} = \bar{N}_0/v_p$, termination rate constants $k_t = 1/(\tau^0_{living} \psi_1^o)$, and rates of polymerization ($R_p = v_p \psi_1^o$), are readily obtained. In the photocopy experiment the dead population is measured simultaneously with the living one. Comparison of the mean dead chain length, $\bar{N}_d$, with the mean living chain length, $\bar{N}_0$, allows the fraction of living chains terminating via disproportionation, f_d, to be extracted. Previously, it was difficult to conceive that one could obtain all these quantities in a single experiment. Results for the FRP of MMA at 60 °C from the photocopy experiment are summarized in the second column of Table 1. These are compared with independent estimates or measurements shown in the third column, and with values reported in the literature, in the fourth column. As can be seen from the entries in the third column of Table 1, calculations of relevant quantities using the known rate of initiation, R_i, independent measurement of the polymerization rate, R_p, and reliable propagation rate constants, v_p, from the literature are, in general, consistent with the quantities measured in the photocopy experiment. Values available in the literature (fourth column) are also in fair agreement with the values obtained in the photocopy experiment.

We hope to extend our living MWD measurements to high conversion FRPs and to more elaborate non-steady-state measurements. Some preliminary yet very promising measurements of time-dependent living chain properties are reported in the accompanying article.[28]

VII. Experimental Section

AIBN (Janssen Chimica) is used as received, and MMA (Aldrich) is purified by passing it through a column ($\cong 2.5$ cm diameter $\times \gtrsim 25$ cm length) filled with inhibitor remover packing (Aldrich #31 134−0). The extinction coefficient of DNPMS is measured by UV absorption to be 2570 M^{-1} cm^{-1} at the photolysis wavelength of 308 nm. With this, the concentration used in the experiments provides an optical density (OD) of $\cong 0.3$ due to the photoinhibitor molecules using

the fused quartz flat sample cells which have a path length of 0.3 cm. The thermal initiator AIBN has an extinction coefficient at 308 nm of $\cong 4$ M^{-1} cm^{-1}; hence, the OD due to AIBN is about 0.01 at the concentrations employed. That is, the ratio OD(AIBN)/OD(DNS) = 0.01/0.3 ≪ 1 is small at the photolysis wavelength and the absorption of light by AIBN is negligible. Similarly, absorption by the monomer MMA is negligible at the photolysis wavelength.

The rate of initiation is[3] $R_i = 2fk_d[init]$, where f is the "efficiency" of the initiator ($\approx 0.5-0.6$ for AIBN[64]), k_d is the first-order thermal decomposition rate of the initiator, and [init] is the initiator concentration. The decomposition rate of AIBN at 60 °C in toluene or benzene is[20] $k_d \cong (0.8-1) \times 10^{-5}$ s^{-1}, providing a rate of initiation $R_i \cong 10^{-7}$ M/s at the initiator concentrations used.

A. Synthesis of Photoinhibitors. A number of compounds were synthesized and tested as potential photoinhibitors. Many of these were discarded due to inefficient cleavage, low solubility, and/or side reactions. Arylmethyl sulfones were found to be the most useful class of compounds as potential photoinhibitors. The synthesis and characterization of photoinhibitor molecules dinaphthyl sulfone (DNS) and di(1-naphthyl, phenyl methyl) sulfone (DNPMS), shown in Figure 2, are discussed in detail in ref 18, where quantum yield measurements for cleavage of the photoinhibitor DNS are also described.

B. Photolysis Setup. The basic photolysis setup is shown in Figure 6. Temperature control is achieved using a variable temperature accessory originally designed for an electron paramagnetic resonance (EPR) instrument (Bruker Instruments ESP 300E). Air flows through a transfer line, where it is heated, then past the sample. A thermocouple placed near the sample relays feedback information to a temperature controller (Bruker Instruments model ER 4111VT) which regulates the current supplied to a heater placed in the transfer line. According to the manufacturer, the temperature regulation is to within ±0.5 °C. However, using a stand-alone thermocouple, it was found that the actual temperature at the sample position is 3−4 °C lower than the temperature set on the controller. All the temperatures quoted in this chapter refer to values set on the controller and not actually measured ones.

The sample cell and the sample insert are made of clear fused quartz (CFQ) using rectangular (3 × 9 and 7 × 13 mm, respectively) tubes from VitroCom, Inc. (Mountain Lakes, NJ). The insert design is based on a standard Bruker insert used for variable temperature EPR studies. Sample cells are fitted with CFQ 8−425 threads taken from EPR tubes (Wilmad Glass, Buena, NJ), such that standard screw caps and PTFE-lined silicone septa can be used.

A Lambda Physik Lasertechnik LEXtra excimer laser is used to photolyze samples (308 nm, 20 ns pulse width). The laser is controlled via a PC, where it is possible to preset the number of pulses to be delivered, as well as pulsing frequencies between 1 and 30 Hz. For pulsing frequencies slower than 1 Hz, an external triggering device (Stanford Research Systems, Inc., model DG535 Digital Delay/Pulse Generator) is used. A lens is employed to diverge the laser beam in order to excite the whole sample uniformly. The resulting laser beam at the sample position was measured using photographic paper to be about 2 cm × 5 cm (cf. the area of the sample facing the laser beam is about 0.9 cm × 0.5 cm). There are no significant changes in the laser intensity per pulse for pulsing rates between 0.05 and 30 Hz.

C. Gel Permeation Chromatography (GPC) Measurements. Our GPC equipment consists of a Kontes Ultra-Ware reservoir fitted with a 5-valve recirculation head, a Knauer WellChrom Mini-Star K-500 A4040 pump (Knauer GmbH, Berlin) fitted with a 10 mL/min pump head, a Rheodyne model 7125 injector with a 200 μL loop, a Groton GTI/SpectroVision FD-500 fluorescence detector (Groton Technology, Inc., Acton, MA), and a Knauer WellChrom K-2300 refractive index detector.

The fluorescence (FL) detector is optimized for high sensitivity. It employs a variable rate, pulsed xenon source (30, 60, or 90 Hz pulse rate) for excitation and a photomultiplier tube
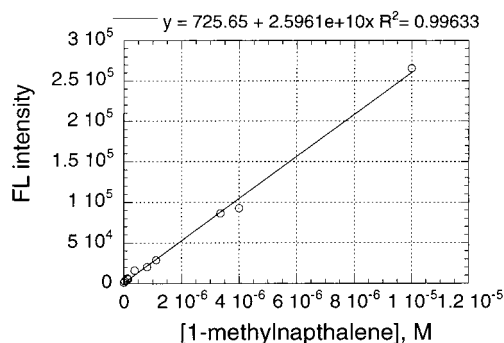

Figure 13. GPC FL detector integrated peak areas as a function of the concentration of the model label 1-methylnaphthalene in THF.
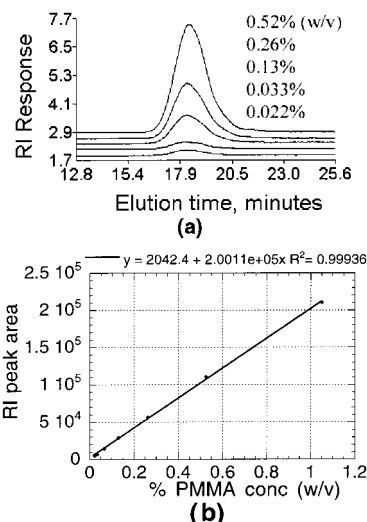

Figure 14. (a) GPC RI chromatograms of PMMA solutions of the indicated concentrations in THF. (b) Integrated peak areas of the chromatograms in (a), plotted as a function of PMMA concentration.

(R268), with a useful detection range from 250 to over 600 nm, for detection of fluorescent energy. A monochromator with a band-pass of 12 nm and another one with a band-pass of 20 nm are used for the excitation and emission sides, respectively. The sample cell is a 24 μL flow cell, and the xenon source is used at 30 Hz pulse rate in all experiments.

Two 300 × 7.5 mm PLgel 5 μm MIXED-C columns, with a linear molecular weight (MW) range of 200−2,000,000, and a 300 × 7.5 mm PLgel 5 μm 100 Å column (resolving range MW ≈ 100−4000) are used in series, with THF as the eluent. The 100 Å column improves the separation at low molecular weights considerably. In earlier experiments, different column sets were tried to find the set which gave the best separation for the systems of interest, all the while maintaining practical elution times. Using the current configuration, at a flow rate of 1 mL/min, each GPC run takes about 35 min.

Data acquisition is performed using a Polymer Laboratories (PL) two channel data capture unit (DCU), connected to the two detectors and to a PC, where data analysis is performed using PL Caliber GPC software.

The MW calibration for both detectors is done using polystyrene standards (PL EasyCal PS-1 Standards Kit), providing a 10 point calibration in the range MW = 580−7 500 000. For the FL detector, fluorescence from polystyrene (PS) is detected with the excitation wavelength set at $\lambda_{ex} = 270$ nm and the emission $\lambda_{em} = 333$ nm. Third-order polynomial fits are used for the elution time vs log MW calibration curves for both detectors.

In addition to MW calibration, the FL detector response (integrated peak areas) is calibrated for the concentration of 1-methylnaphthalene, a model compound for labeled dead

chains (λ_{ex} = 300 nm, λ_{em} = 350 nm, Figure 13), and the RI detector response is calibrated for PMMA concentration (Figure 14).

D. Accumulating Labeled Dead Copies. Repeating the photocopy process to accumulate labeled dead copies of the living MWD improves signal intensities. However, one must be careful about photoinhibitor depletion and formation of products which might interfere with the photocopying process. These effects can be checked by plotting the response of the FL detector (integrated areas under chromatogram peaks) as a function of the number of laser shots accumulated. Such plots are linear up to about 20 shots for the photoinhibitor DNPMS. Thus, in all experiments reported here the number of laser shots is kept ≤ 20, unless noted otherwise.

References and Notes

(1) Odian, G. *Principles of Polymerization*; John Wiley and Sons: New York, 1981.
(2) Committee on Polymer Science and Engineering; Board on Chemical Sciences and Technology; Commission on Physical Sciences, Mathematics, and Applications In *Polymer Science and Engineering: The Shifting Research Frontiers*; National Academy Press: Washington, D. C. 1994; p 16.
(3) Flory, P. *Principles of Polymer Chemistry*; Cornell University Press: Ithaca, NY, 1971.
(4) Bamford, C. H. Radical Polymerization. In *Encyclopaedia of Polymer Science and Engineering*; Marks, H. F., Bikales, N. M., Overberger, C. G., Menges, G., Kraschwitz, J. I., Eds.; John Wiley & Sons: New York, 1985; Vol. 13.
(5) Rempp, P.; Merrill, E. *Polymer Synthesis*; Huethig & Wepf: New York, 1986.
(6) Bamford, C. H.; Barb, W. G.; Jenkins, A. D.; Onyon, P. F. *The Kinetics of Vinyl Polymerization by radical Mechanisms*; Butterworth: London, 1958.
(7) Morawetz, H. *Polymers, the Origins and Growth of a Science*; John Wiley & Sons: New York, 1985.
(8) Benson, S. W.; North, A. M. *J. Am. Chem. Soc.* **1962**, *84*, 935−940.
(9) Ito, K. *J. Polym. Sci.: Polym. Chem. Ed.* **1974**, *12*, 1991−2004.
(10) Mahabadi, H.-K. *Macromolecules* **1985**, *18*, 1319−1324.
(11) Mahabadi, H.-K. *Macromolecules* **1991**, *24*, 606−609.
(12) Cardenas, J.; O'Driscoll, K. F. *J. Polym. Sci., Polym. Chem. Ed.* **1976**, *14*, 883−897.
(13) Tulig, T. J.; Tirrell, M. *Macromolecules* **1981**, *14*, 1501−1511.
(14) Tulig, T. J.; Tirrell, M. *Macromolecules* **1982**, *15*, 459−463.
(15) Russell, G. T.; Napper, D. H.; Gilbert, G. *Macromolecules* **1988**, *21*, 2133-2140.
(16) Moad, G.; Solomon, D. H. *The Chemistry of Free Radical Polymerization*; Elsevier Science: Tarrytown, NY, 1995.
(17) Balke, S. T.; Hamielec, A. E. *J. Appl. Polym. Sci.* **1973**, *17*, 905−949.
(18) Karatekin, E. Dynamics of Free Radical Polymerization. Ph.D. Thesis Columbia University New York, 1999.
(19) Friedman, B.; O'Shaughnessy, B. *Europhys. Lett.* **1993**, *23*, 667; *Macromolecules* **1993**, *26*, 5726.
(20) Brandrup, J.; Immergut, E. H.; Grulke, E. A.; Abe, A.; Bloch, D. R. *Polymer Handbook*, 4th ed.; Wiley: New York, 1999.
(21) Holdcroft, S.; Yuen, K. H.; Guillet, J. E. *J. Polym. Sci.: Part A: Polym. Chem.* **1990**, *28*, 1495−1505.
(22) Holdcroft, S.; Guillet, J. E. *J. Polym. Sci.: Part A: Polym. Chem.* **1991**, *29*, 729−737.

(23) Holdcroft, S.; Tang, B.-Z.; Guillet, J. E. *J. Chem. Soc., Chem. Commun.* **1991**, 280−282.
(24) Holdcroft, S.; Guillet, J. E. *Macromolecules* **1991**, *24*, 1210−1212.
(25) Tang, B.-Z.; Holdcroft, S.; Guillet, J. E. *Macromolecules* **1994**, *27*, 5487−5490.
(26) Modi, P. J.; Guillet, J. E. *J. Photochem. Photobiol. A: Chem.* **1994**, *84*, 213−220.
(27) O'Shaughnessy, B. (2001, preprint).
(28) Karatekin, E.; Landis, M.; Lem, G.; O'Shaughnessy, B.; Turro, N. J. *Macromolecules* **2001**, *34*, 8202.
(29) Schulz, G. V.; Husemann, F. *Z. Phys. Chem. B* **1937**, *36*, 183.
(30) North, A. M.; Reed, G. A. *Trans. Faraday Soc.* **1961**, *57*, 859−870.
(31) O'Driscoll, K. F.; Mahabadi, H. K. *J. Polym. Sci.: Polym. Chem. Ed.* **1976**, *14*, 869−881.
(32) Mita, I.; Horie, K. *J. Macromol. Sci., Rev. Macromol. Chem. Phys.* **1987**, *C27* (1), 91−169.
(33) O'Shaughnessy, B.; Yu, J. *Phys. Rev. Lett.* **1994**, *73*, 1723−1726.
(34) O'Shaughnessy, B.; Yu, J. *Macromolecules* **1994**, *27*, 5067−5078.
(35) O'Shaughnessy, B.; Yu, J. *Macromolecules* **1994**, *27*, 5079−5085.
(36) Mita, I.; Horie, K.; Takeda, M. *Macromolecules* **1981**, *14*, 1428.
(37) Gebert, M. S.; Torkelson, J. M. *Polymer* **1990**, *31*, 2402.
(38) Wisnudel, M. D.; Torkelson, J. M. *J. Polym. Sci., Polym. Phys. Ed.* **1996**, *34*, 2999.
(39) de Gennes, P. G. *Scaling Concepts in Polymer Physics*; Cornell University Press: Ithaca, NY, 1985.
(40) Doi, M. *Chem. Phys.* **1975**, *11*, 107−113, 115−121.
(41) O'Shaughnessy, B. *Macromol. Theory Simul.* **1995**, *4*, 481−496.
(42) Gebert, M. S.; Yu, D. H. S.; Torkelson, J. M. *Macromolecules* **1992**, *25*, 5, 4160.
(43) Yu, D. H.; Torkelson, J. M. *Macromolecules* **1988**, *21*, 852.
(44) Horie, K.; Schnabel, W.; Mita, I.; Ushiki, H. *Macromolecules* **1981**, *14*, 1422.
(45) Johnston, L. J.; Scaiano, J. C. *J. Am. Chem. Soc.* **1985**, *107*, 6368−6372.
(46) Yau, W. W.; Kirkland, J. J.; Bly, D. D. *Modern Size-Exclusion Liquid Chromatography: Practice of Gel Permeation and Gel Filtration Chromatography*; Wiley: New York, 1970.
(47) Karatekin, E.; O'Shaughnessy, B.; Turro, N. J. *Theory of Photocopying Living Chain Distributions*; 2001; in preparation.
(48) Ranby, B.; Rabek, J. F. *ESR Spectroscopy in Polymer Research*; Springer-Verlag: Berlin, 1977.
(49) Kamachi, M. *Adv. Polym. Sci.* **1987**, *82*, 207−275.
(50) Bresler, S. E.; Kazbekov, E. N.; Shadrin, V. N. *Makromol. Chem.* **1974**, *175*, 2875.
(51) Kamachi, M.; Kohno, M.; Kuwae, Y.; Nozakura, S.-I. *Polym. J.* **1982**, *14*, 749−752.
(52) Turro, N. J. *Modern Molecular Photochemistry*; University Science Books: Mill Valley, CA, 1991.
(53) Hutchinson, R. A.; Aronson, M. T.; Richards, J. R. *Macromolecules* **1993**, *26*, 6410−6415.
(54) Birks, J. B. *Photophysics of Aromatic Molecules*; Wiley-Interscience: London, 1970.
(55) Nevertheless some broadening due to the abovementioned effects and/or instrumental settings may still be significant, since the polydispersity obtained from the RI detector is consistent with disproportionation dominated termination (PD$_{dead}$ ≅ 2.0, assuming k_t is *independent of N*, ref 5), while comparison of mean living vs dead chain lengths suggest less than half the chains terminate via disproportionation.
(56) Brandrup, J.; Immergut, E. H. *Polymer Handbook*, 3rd ed.; Wiley: New York, 1966; Chapter V (Physical Constants of Poly(methyl methacrylate)), p 78.
(57) Zammit, M. D.; Davis, T. P.; Haddleton, D. M.; Suddaby, K. G. *Macromolecules* **1997**, *30*, 1915−1920.
(58) Friedman, B.; O'Shaughnessy, B. *Int. J. Mod. Phys. B* **1994**, *8*, 2555−2591.
(59) O'Shaughnessy, B. *Phys. Rev. Lett.* **1993**, *71*, 3331−3334.
(60) O'Shaughnessy, B. *Macromolecules* **1994**, *27*, 3875−3884.
(61) Jockusch, S.; Turro, N. J. *J. Am. Chem. Soc.* **1998**, *120*, 11773−11777.
(62) Jockusch, S.; Turro, N. J. *J. Am. Chem. Soc.* **1999**, *121*, 3921−3925.
(63) Martschke, R.; Farley, R. D.; Fischer, H. *Helv. Chim. Acta* **1997**, *80*, 1363−1374.
(64) Watanabe, Y.; Ishigaki, H.; Ikada, H.; Suyama, S. *Polym. J.* **1997**, *29*, 733−736.